Heliyon 8 (2022) e10799

Contents lists available at ScienceDirect

Heliyon

journal homepage: www.cell.com/heliyon

Research article

Kinetics of Benzo(a)pyrene biodegradation and bacterial growth in sandy soil by *Sphingobacterium spiritovorum*

Salina Alias [a,*], Megawati Omar [b], Noor Hana Hussain [c], Nor Amani Filzah Mohd-Kamil [d], Suhaimi Abdul-Talib [e]

[a] Centre for Civil Engineering Studies, Universiti Teknologi MARA, Cawangan Pulau Pinang, Permatang Pauh Branch, 13500 Seberang Prai, Pulau Pinang, Malaysia
[b] Academy of Languages Studies, Universiti Teknologi MARA, 40450 Shah Alam Selangor, Malaysia
[c] Institute of Science, Universiti Teknologi MARA, 40450 Shah Alam Selangor, Malaysia
[d] Faculty of Civil and Environmental Engineering, Universiti Tun Hussein Onn, 86400 Batu Pahat, Johor, Malaysia
[e] School of Civil Engineering, College of Engineering, Universiti Teknologi MARA, 40450 Shah Alam Selangor, Malaysia

ARTICLE INFO

Keywords:
Benzo(a)pyrene
Biodegradation
Monod
Polycyclic aromatic hydrocarbon (PAH)
Sphingobacterium

ABSTRACT

Biodegradation is the economically viable solution to restore land contaminated by hazardous pollutants such as benzo(a)pyrene (BaP). The present study focuses on the biodegradation of benzo(a)pyrene by *Sphingobacterium spiritovorum* in contaminated soil. The biodegradation kinetics and bacterial growth were evaluated while the biokinetic model that described the benzo(a)pyrene biodegradation was established. The Monod, Haldane, Powell and Edward models were used to model the bacterial growth in benzo(a)pyrene contaminated soil. Excel template was developed with Fourth order Runga-Kutta numerical algorithm to find the biokinetic parameters of the complex non-linear regression model. An Excel Solver function was used to obtain reasonable best-fit values of kinetic parameters. The Haldane and Edward models are well fit to describe the growth trend and model the kinetics of benzo(a)pyrene biodegradation. Enzyme substrate inhibition is the critical factor that affects the benzo(a)pyrene degradation by *S. spiritovorum,* which the model defines physically. The results demonstrated that removing benzo(a)pyrene showed positive interaction between substrate inhibition, the concentration of benzo(a)pyrene and sorption of the contaminants on soil particles.

1. Introduction

Sustainable land restoration is urgently needed, especially for an area with limited productive land and funds to restore the contaminated lands are scarce. Land contamination and deterioration cause plenty of losses in the economy as they are unable the utilisation of productive land. In reality, land contamination endangers water supplies, puts groundwater reservoirs at risk, exposes people to health concerns, pollutes the environment, and disturbs the ecological system's natural balance (Thakur et al., 2022; Dai et al., 2022). Additionally, the contaminated land has reduced soil fertility, resulting in lower agricultural yield and the production of contaminated and unsafe food (Dai et al., 2022; Saravanakumar et al., 2022; Wang et al., 2021).

Polycyclic aromatic hydrocarbon (PAH) is one of organic compound that has been identified as the concern soil contaminants due its toxicity, carcinogenic and mutagenic behaviour. It is widespread and can present in more than 100 different combinations. However, the United States Environmental Protection Agency (USEPA) has only listed 16 PAHs as priority contaminants due to their potential danger to human health. One of the most dangerous priority PAHs, benzo(a)pyrene (BaP), a high molecular weight PAH (HMW-PAH) has been shown to have a negative impact on prenatal development, cancer risk, and children's cognitive and genetic health (Perera et al., 2005; Plísková et al., 2005; Gonçalves et al., 2008). With its five benzene rings arranged in an angular pattern and poor solubility (3.8 ug/L), benzo(a)pyrene is less accessible to biochemical and nucleophilic processes, making it more difficult to remove from contaminated soils (Wick et al., 2011). As per Canadian Council of Ministers of the Environment (Canadian Council of Ministers of the Environment, 2010) and Department of Environment Malaysia (DOE, 2009), the permissible limit of benzo(a)pyrene in residential and industrial soil is within the range 0.015–0.7 mg/kg and 0.7–2.1 mg/kg respectively. Aside, the tolerable limit for benzo(a)pyrene in agricultural soil is 0.1 mg/kg (Canadian Council of Ministers of the Environment, 2010).

* Corresponding author.
E-mail address: salina346@uitm.edu.my (S. Alias).

https://doi.org/10.1016/j.heliyon.2022.e10799
Received 15 June 2022; Received in revised form 23 August 2022; Accepted 23 September 2022

Numerous bacterial degraders with the capacity to clean up PAH-contaminated sites, including *Bacillus sp., Pseudomonas, Sphingomonas sp., Ochrobactrum sp., Mycobacterium, Paracoccus, and Sphingobacterium sp.*, have been identified from various environments (Su et al., 2021; Lu et al., 2021; Sahar et al., 2020; Smu et al., 2020; Sanghvi, 2005;Janbandhu and Fulekar, 2011). These microbes were isolated from varied locations, enriched in various substrates, and demonstrated varying capacity for biodegradation the PAHs. *Sphingobacterium* is among the PAH degrader that was isolated from soil and marine ecosystem polluted by petroleum-based chemical (Janbandhu and Fulekar, 2011). The genus is also ubiquitous in nature as it has been isolated in many environments such as different soil types, stagnant water, compost, wastewater sludge, plants, human blood and human clinical specimen (Hibi and Kumano, 2017; Lambiase et al., 2009; Tronel et al., 2003; Jørgensen et al., 2000).

Currently, most existing biodegradation studies are limited to laboratory experiments within the low-molecular-weight PAH (LMW-PAH) degradation, mixed PAH of LMW and HMW, and mixed cultures (Sun et al., 2022; Mu et al., 2022; Liang et al., 2022). However, data on biodegradation kinetics, prediction of the remaining concentrations from the PAH degradation and microbial growth are still limited. Information in degradation kinetics is necessary to comprehend the behaviour of PAHs in soils and scale up PAH contaminated soil remediation strategies. Several kinetics model in biodegradation that associated with non-growing organism (i.e. first order, second order), growing organism (i.e. Monod, Logistic) and substrate-inhibition (i.e Edward, Haldene) can be used to estimate the biodegradation kinetics parameters (Priyadarshini et al., 2021). The accuracy and reliability of the estimated model parameters is important to assess the prospect of remediation strategy which can save time and cost.

Therefore, this study aims to examine the reliability of the models by comparing with the experimental data and select the appropriate model to best describe the biodegradation reaction. The *Sphingobacterium spiritovorum* is used as degrader in remediating benzo(a)pyrene contaminated soil. In order to make predictions about the benzo(a)pyrene degradation by *S. spiritovorum* more conveniently, the growth and degradation kinetics models is developed using the Excel with solver function.

2. Materials and methods

2.1. Preparation of Spiked-benzo(a)pyrene contaminated sand

In this study, a spiked sand was used in which the sand was artificially contaminated with benzo(a)pyrene. Therefore, in order to hinder any interference of growth substrate or cometabolism effect, the presence of indigenous PAHs in soil was analysed for the exclusively examined the spiked BaP as a solely substrate for microorganism growth. The preliminary studied showed the sand was free from any presence of 16PAHs such as benzo(a)pyrene, anthracene and phenanthrene as shown in Table 1. The sand with the granulometric composition of 99.94% sand and 0.06% silt with clay was used in this study.

Table 1. Physical and chemical properties of sand.

Sand Properties	Remarks
Sand (%)	99.94
Silt and Clay (%)	0.06
pH	6.23 ± 0.3
Water Holding Capacity (mL/30 g of sand)	0.27%
Moisture Content (%)	2
Type of Sand	Silica Sand
CHNS (%)	0.08:0.001:0:0
PAHs Content (mg/kg dry sand)	
Anthracene	nd
Phenanthrene	nd
Benzo(a)pyrene	nd

nd – not detected.

In the preparation of spiked sand of 100 mg benzo(a)pyrene/kg sand, 20-g dried sand was transferred into a conical flask and spiked with 20-mL benzo(a)pyrene-acetone solution at a concentration of 100 mg BaP/L of acetone (Alias et al., 2012). The spiked sand was agitated for two weeks at 150 rpm using an orbital shaker (Multitron Standard, Infors HT, Switzerland) to evaporate the solvent, aging period and ensure a better distribution of benzo(a)pyrene in the sand. Three replicates were performed for each sand sample. The 30, 70, 125 and 150 mg/kg benzo(a)pyrene/kg sand was also prepared through the same approach. This number was established in accordance with a literature analysis, which revealed that the range of benzo(a)pyrene concentrations from different sites is between 0.002 and 143 mg/kg soil.

2.2. Reviving and sub-culturing of bacteria

The *S. spiritovorum* which was preserved at -80 °C in microbeads (microbank™), had been revived by aseptically transferring the beads into a nutrient broth, NB (Merck), pH 7.0 ± 0.2 and left to grow at 30 ± 2 °C in a static incubator (Lovibond, Germany). The strain had been isolated from municipal sludge in part of the unreported work by Othman et al. (2010). After a lag phase, the nutrient broth turned turbid indicating that the bacteria had grown in the broth. The broth cultures were then streaked on nutrient agar (Oxoid) plates using a sterilised loops quadrant streaking technique. The plates were then incubated in an inverted position in a static incubator (Lovibond, Germany) at 30 ± 2 °C for five days.

A loop-full of a single bacterial colony from these agar plates was taken and re-streaked onto a new nutrient agar plate. It was then incubated at 30 ± 2 °C for five days. The sub-culturing was repeated another two times to ensure the purity and revive of the bacteria strains. A purified colony of the bacteria was taken using a sterilised loop and transferred into 50 mL sterilised nutrient broth (Merck). The broth culture was incubated in a static incubator (Lovibond, Germany) at 30 ± 2 °C. All microbiological works were conducted in a Biological Safety Cabinet, Class II (NuAire Labgard, USA).

2.3. Volume of active bacteria culture (VABC)

Bacteria population of approximately 10^8 colonies per gram of soil (CFU/g) was chosen as the concentration of inoculums to be inoculated in this study. This was performed by carrying out a series of 10-fold serial dilution (10^1–10^{10}) from a one mL broth culture at mid-exponential phase into 9 mL sterile phosphate buffer saline solution (PBS) as diluent (Lammert, 2007). The PBS solution contained Na_2HPO_4 (8.5 g/L), KH_2PO_4 (3 g/L), NaCl (0.5 g/L) and KI (0.001 g/L).

At each transfer, the bacterial suspension was thoroughly mixed using a vortex mixture. A 200 μL of each dilution aliquot was pipetted onto nutrient agar plates and spread evenly using a sterile disposable L-shape spreader. The plates were incubated in an inverted position at 30 °C ± 2 °C for five days. The colonies formed on the agar plates were enumerated and expressed as colony-forming units per culture (CFU/mL). Eq. (1) was used to calculate the number of colonies present in the culture. Subsequently, the volume of the bacteria culture that would contain ca. 10^8 CFU/g of soil was determined using Eq. (2). This volume was referred as the volume of active bacteria culture (VABC). The VABC was centrifuged for 15 min at 5000 rpm and suspended in 2-mL sterilised minimal media solution (MMS), which contains Na_2HPO_4 (8.5 g/L), KH_2PO_4 (3 g/L), NaCl (0.5 g/L), NH_4Cl (1 g/L), $MSO_4.7H_2O$ (0.5 g/L), $CaCl_2$ (0.0147 g/L), $CuSO_4$ (0.0004 g/L), KI (0.001 g/L), $MnSO_4.H_2O$ (0.004 g/L), $ZnSO_4$ (0.004 g/L), H_3BO_3 (0.005 g/L), $FeCl_3$ (0.002 g/L) and pH 7.0 ± 0.2. The suspension was used in the biodegradation experiments.

$$\textit{Bacterial Count in culture},\ C\left(\frac{CFU}{mL}\right) = \frac{N \text{ x } DF}{V} \text{ x } 1000 \quad (1)$$

where N is the number of counted colonies, DF is the dilution factor (from 10^1-10^{10}) and V is the volume of inoculums that was inoculated on agar plates, e.g. 200 uL (uL).

$$\textit{Volume of Active Bacteria Culture},\ VABC\ (mL) = \frac{(1 \text{ x } 10^8)\ M}{C} \quad (2)$$

where C is the microbial count in 1 mL of culture (CFU/mL) from Equation (1) and M is the total weight of sand in the flask containing PAH-spiked sand (20 g).

2.4. Biodegradation experiment

The biodegradation experiment was set up by inoculating a predetermined VABC (culture in 2-mL MMS). This will result in a biological reactor with 20 g of sterilised spiking benzo(a)pyrene sand having approximately 10^8 CFU/g of soil of initial microbial concentration. Prior to the culture inoculation, 11 mL of sterile MMS were added to each flask reactor as inorganic nutrition sources for the bacteria. While the control flask reactors were made by adding 13 mL of sterile MMS to another conical flask filled with sand contaminated with BaP. Notably, the control samples received no bacterial culture inoculation. Since moisture can limit microbial activity, a moisture content of 60% was maintained throughout the biodegradation experiment. Therefore, by adding a volume of 13 mL of MMS at the beginning of the experiment had increased the soil water content from 2% (Table 1) to 60%. To compensate for lost moisture in the biological and control reactors, an addition of 0.2 mL sterilised MMS was made each day. All the chemicals used for MMS were purchased from R&M except for Na_2HPO_4 (Fisher Scientific) and KH_2PO_4 (Univar). Then, the biodegradation and controls samples in the flask reactor were incubated in an incubator shaker (Multitron Standard, Infors HT, Switzerland) at 30 ± 2 °C and 150 rpm. Fixed intervals of time were set aside each day to sample the sand from each flask using a sterile spatula for the benzo(a)pyrene analyses and bacteria enumeration. Figure 1 shows the schematic diagram of biodegradation experiment that involves sample preparation, incubation, bacterial enumeration, and benzo(a)pyrene analysis.

2.5. Benzo(a)pyrene analyses and bacteria enumeration in sand

The sampled soil was then accurately weighed to 0.5 g for the benzo(a)pyrene concentration analysis. At the same time, 0.2 g sand was aseptically transferred into a 10 mL phosphate buffer solution (PBS) for bacterial enumeration. Following a serial dilution method and a 5-day incubation, the colonies grown on the agar plate were enumerated. The number of viable colonies was determined and bacterial count in soil which was expressed by colony-forming unit per gram of soil (CFU/g) is calculated using Eq. (3).

$$\textit{Bacterial Countinsoil},\ S\left(\frac{CFU}{g}\right) = \frac{\frac{N \text{ x } DF}{V} \text{ x } 1000}{m} \quad (3)$$

where N is the number of counted colonies, DF is the dilution factor (from 10^1-10^{10}), V is the volume of inoculums that was inoculated on agar plates, e.g. 200 uL and M is the weight of sampled sand in gram (0.2 g).

The benzo(a)pyrene concentration in sand sample was analysed using a High-Performance Liquid Chromatograph (HPLC), which was equipped with a UV detector after extracted using a Microwave-Assisted Extraction (MAE) system (Multiwave 3000, AntonPaar, Austria) and concentrated using a rotary evaporator at a set temperature of 45 °C (Rotavapor system®, Buchi, Switzerland). In the extraction, 25-mL hexane and acetone solutions (AR grade, MERCK) at a ratio of 7:3 was used and the MAE system with 8SXF100 rotor was set to operate at 120 °C for 10 min where the pressure was increased at 0.5 bar/s and then maintained at 10 bar s until 40 min. The extraction procedure was in compliance to the USEPA Method 3546: Microwave Extraction (USEPA, 2007). The procedure described in USEPA Method 3500C: Organic Extraction and Sample Preparation (USEPA, 2007) was also followed for the benzo(a)pyrene extraction.

In the HPLC analysis, the pump was configured to equilibrate at 3 min with the setting of the mobile phase at acetonitrile (ACN) to water ratio of 55:45 and a flow rate of 1.0 mL/min. Then the pump was gradually increased to flow at 1.2 m/min in 6 min with the same ratio of ACN:-water. The eluting strength of the mobile phase was then increased to 75:25 ratio (ACN:water) for another 6 min of the analysis with the flow rate of 1.2 mL/min. The configuration took 19 min to obtain a complete analysis of the analyte and this setting was applicable to each analyte analysis. The UV/VIS detector (Series 200, PerkinElmer, USA) at wavelength of 254 nm was employed to detect the benzo(a)pyere compound.

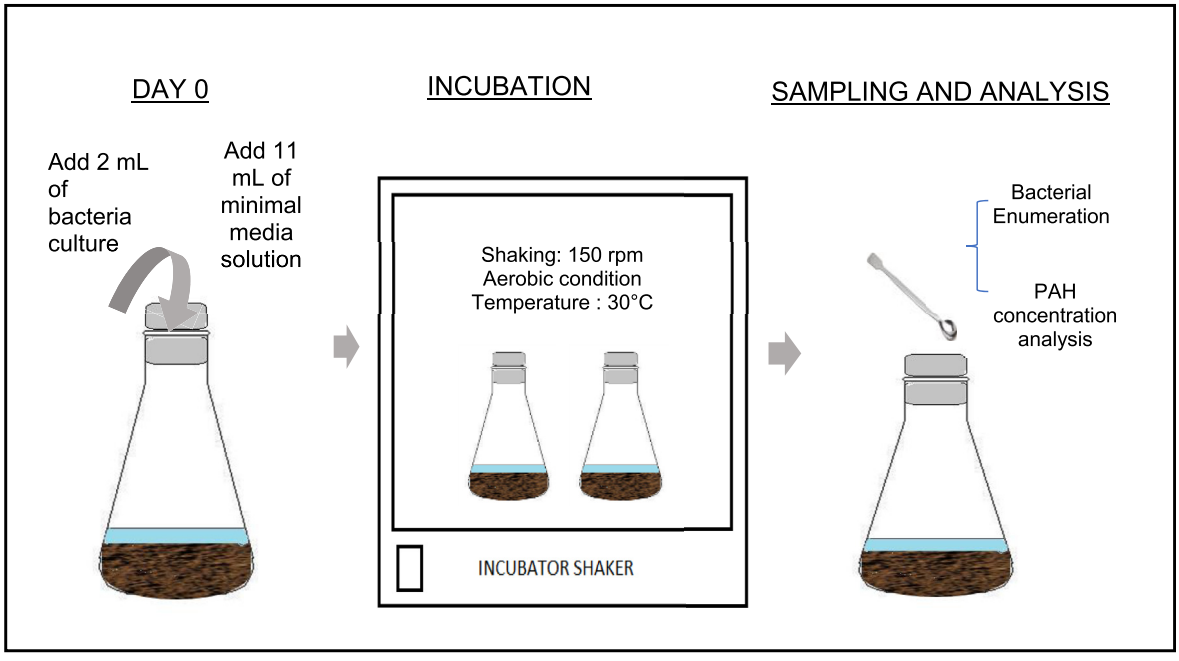

Figure 1. Schematic diagram of biodegradation experiment.

TotalChrome Navigator software (TCNav) was used for the configuration of the HPLC system. The benzo(a)pyrene standard solution of 1000 mg/L (Supelco, USA) was purchased and used as calibration standard. All the analyses using HPLC was performed according to US EPA Method 8310: Polycyclic Aromatic Hydrocarbon (USEPA, 1986) and USEPA Method 8000C: Determinative Chromatographic Separations (USEPA, 2003) procedures. Figure 2 summaries the process flow of benzo(a)pyrene analysis from sand sample and bacteria enumeration. Eq. (4) was used to calculate the benzo(a)pyrene concentration in the sand sample.

$$\text{Concentration of BaP in the sand sample, } C_s \text{ (mg/kg)} = \frac{AV_t}{CF_{mean}CW} \quad (4)$$

Where A is the area under chromatograph peak of BaP, V_t is the volume of concentrated extract (1 mL), CF_{mean} is the mean of calibration factor that is obtained from mean of peak area of the standard BaP solutions at relative standard deviation not more than 20%. W is the weight of sand sample for extraction (0.5 g) and C is the mass of the BaP analyte injected (5 μL).

2.6. Modelling for S. spiritovorum growth

The Monod, Haldane, Edward and Powell models were used to simulate the predicted *S. spiritovorum* growth in soil when benzo(a)pyrene was used as a single substrate at different initial substrate concentrations of 30, 70, 100, 125 and 150 mg/kg of soil. Prior to the simulation of bacterial growth using the models, the specific bacterial growth rate, μ (Equation 5), in the exponential growth phase was determined. The μ at each substrate concentration was plotted versus the concentration of substrate. Then it was model using Monod (Equation 6), Haldane

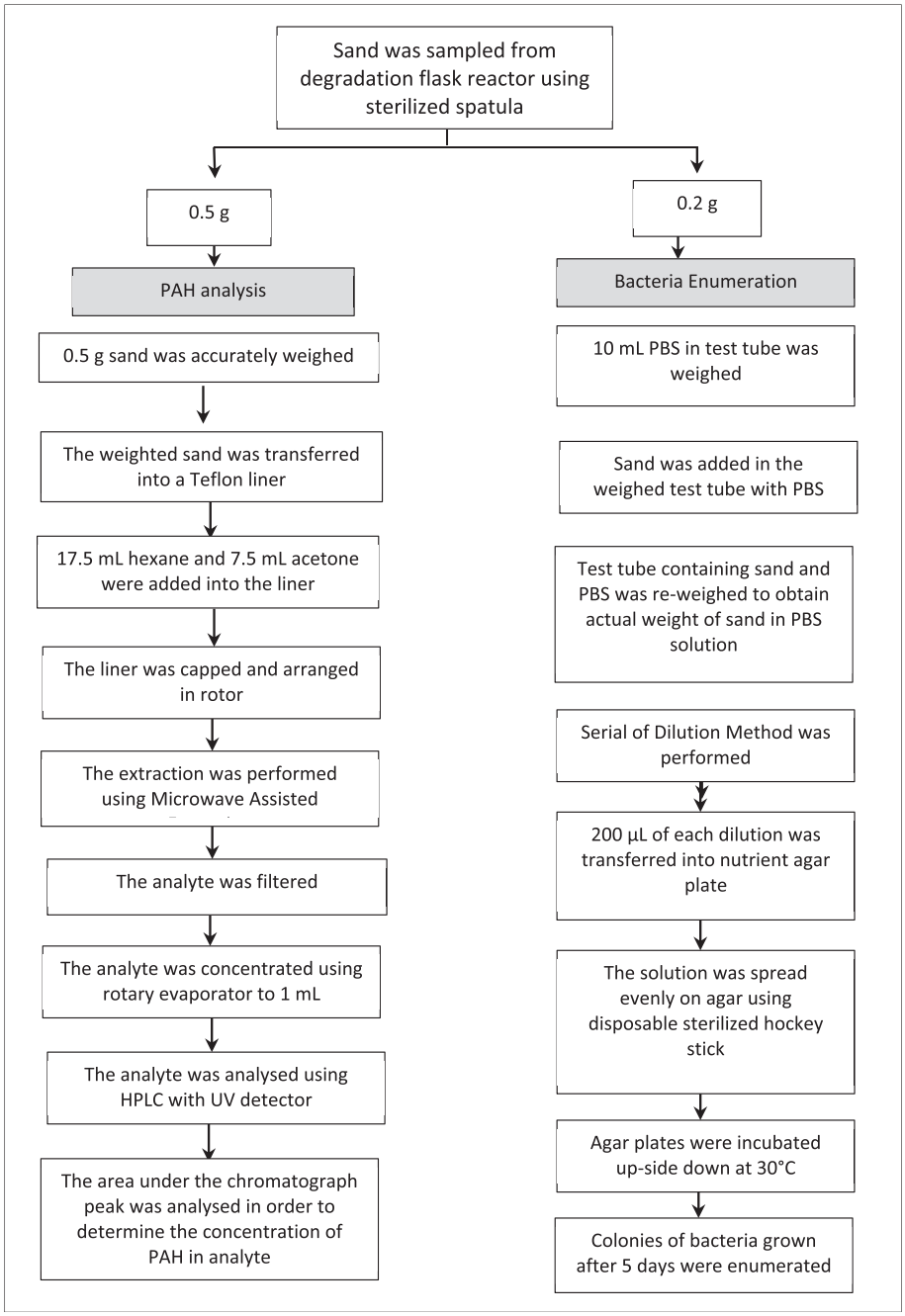

Figure 2. Process flow of sand sample analysis.

Table 2. Model simulation for bacterial growth and substrate utilization (Muloiwa et al., 2020).

Parameters	Model Equations	Equation	Nomenclature
Specific bacterial growth rate, μ	$\mu = \frac{ln\left(\frac{X_2}{X_1}\right)}{t_2 - t_1}$	Eq. (5)	X = biomass concentration (CFU/kg) t = time (day)
Monod Model		Eq. (6)	μ = specific growth rate of bacteria (day-1)
Haldane Model	$\mu = \frac{\mu_{max} S}{K_s + S}$	Eq. (7)	μ_{max} = maximum specific growth rate of bacteria (day-1)
Powell Model	$\mu = \frac{\mu_{max} S}{K_s + S + \frac{S^2}{K_i}}$	Eq. (8)	S = Sorb substrate concentration in soil (mg/kg)
Edward Model	$\mu = \frac{(\mu_{max} + m)S}{K_s + S} - m$	Eq. (9)	K_s = half saturation constant of substrate (mg/kg) k_i = substrate inhibition coefficient (mg/kg)
Substrate utilization, (mg/kg)	$\mu = \frac{\mu_{max} S}{K_s + S + \left(\frac{S^2}{K_i}\right)\left(1 + \frac{S}{K}\right)}$	Eq. (10)	q_{max} = maximum substrate utilization rate per biomass concentration (mg/mg/d) k_b = First order rate coefficient for desorption of substrate from soil (1/day) S_s = concentration of solubilized substrate (desorb) in liquid phase (mg/kg) m is maintenance rate (day^{-1}) and 1 + S/K is additional term in denominator where K is constant
	$\frac{dS}{dt} = k_b S - \frac{q_{max} S_s X}{k_s + S_s + \frac{S_s^2}{k_i}}$		

(Equation 7), Powell (Equation 8) and Edward (Equation 9) models as model equation shown in Table 2. The model parameters, namely, μ_{max}, k_s, k_i, m and 1 + S/K were set as fitting variables and their uncertainties were estimated through the best curve fit of the non-linear regression with the observed data.

2.7. Model simulation for BaP biodegradation kinetics

Fourth order Runga-Kutta numerical algorithm was used to find the uncertainties of the complex non-linear regression through the developed an Excel spreadsheet template for benzo(a)pyrene removal or substrate utilisation rate (Equation 10) in biodegradation by *S. spiritovorum*. An Excel Solver function was used to obtain reasonable best-fit values of kinetic parameters based on the minimum target objective of sum square error (SSE) between observed and predicted data. After several iteration processes, the prediction data and goodness of fit model parameter values were obtained. The substrate utilisation model using Eq. (10) that incorporate first-order kinetics on the desorption of benzo(a)pyrene from the soil particles and biodegradation models that fit either Eqs. (6), (7), (8), and (9) were used in this study. The desorption and biodegradation models were also used to describe the decrease in diesel concentration in the soil phase (Balseiro-Romero et al., 2019). The model parameters, namely, q_{max}, k_b and X were set as fitting variables and their uncertainties were estimated through the best curve fit of the non-linear regression with the observed data.

The validity of the proposed model was evaluated to estimate the accuracy of the prediction model function in practice by comparing the prediction data and the observation data. The model was validated by performing a statistical analysis between the observation data (experiment) and prediction data. The difference between the observed concentrations (C_{obs}) and the predicted concentrations (C_{pred}) data was calculated by minimising the value of sum square error (SSE) indicates the closeness between the observation and prediction data. In addition, a well-fit between the observation and prediction data can also be indicated by the coefficient of determination (R^2). The two-tailed Student's t-distribution (probability and degree of freedom) and 95% confidence interval (CI) between the observation and prediction data were also indicated in the developed Excel template.

3. Results and discussions

3.1. Modelling the S. spiritovorum growth in Benzo(a)pyrene environment

The *S. spiritovorum* growth in sandy soil in different benzo(a)pyrene concentrations are shown in Figure 3. The period of the exponential

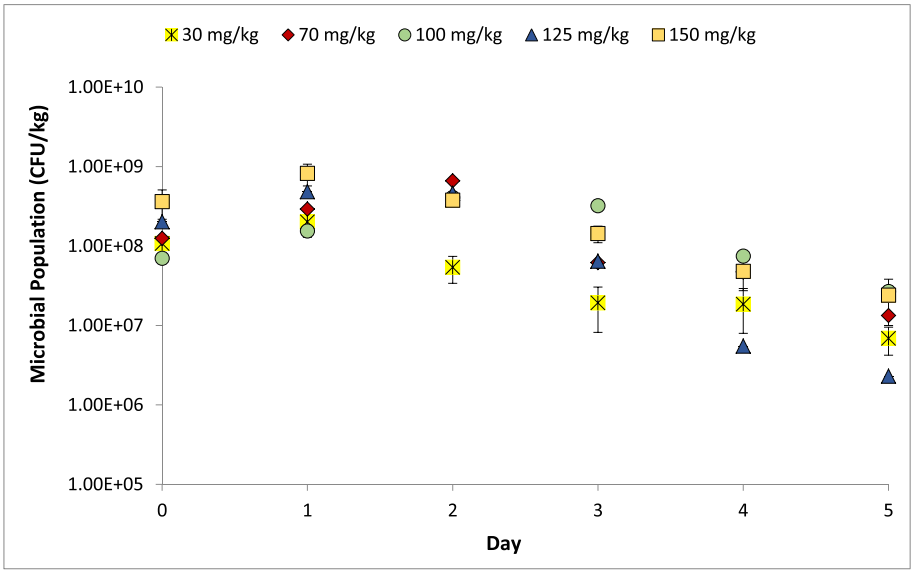

Figure 3. Growth Trend of *S. spiritovorum* in benzo(a)pyrene of Different Concentrations.

Table 3. Specific bacteria growth rate at different substrate initial concentration.

Parameter	Initial BaP Concentration (mg/kg)				
Specific bacterial growth rate, μ (day^{-1}) **(This study)**	30 mg/kg	70 mg/kg	100 mg/kg	125 mg/kg	150 mg/kg
	0.6304 ±0.193	0.8296 ± 0.069	0.8811 ± 0.146	0.8719 ± 0.122	0.7557 ± 0.11
	Initial carbazole (nitrogen heterocyclic PAH) concentration (mg/L)				
Specific bacterial growth rate, μ (day^{-1}) (Ghosh and Mukherji, 2020)	25	50	100	200	300
	0.96	1.12	1.48	1.62	1.91

growth phase varied depending on the initial benzo(a)pyrene concentrations. At high benzo(a)pyrene concentration, the bacterium replicated rapidly compared to low PAH (substrate) concentration. The *S. spiritovorum* increased from 2.6 × 10^8 CFU/kg to 1.1 × 10^9 CFU/kg within one day at the initial benzo(a)pyrene concentration of 150 mg/kg. At this initial concentration, the specific growth rate (μ) was measured at 0.7557 day^{-1} (Eq. 5). Meanwhile, the growth increase to 2.0 × 10^8 CFU/kg from 1.0 × 10^8 CFU/kg at 30 mg/kg initial benzo(a)pyrene concentration with μ = 0.6304 day^{-1}. The bacterium expanded six times during the exponential phase at the initial benzo(a)pyrene concentration of 100 mg/kg, resulting in the greatest specific growth rate (μ) = 0.8811 ± 0.146 day^{-1}. Zeneli et al. (2019) observed that throughout the biodegradation of PAHs, the numbers of inoculated bacteria in soil increased by three times. However, a very modest growth (1.6%) was noted in the final 20 days of the experiment. On the other hand, a 10 fold increase of bacterial strain from 10^{10} to 10^{11} was observed with μ = 0.06 h^{-1} to remediate biodiesel contaminated soil (Balseiro-Romero et al., 2019).

Variations in the specific growth rate with respect to the initial benzo(a)pyrene concentration are summarised in Table 3. It is evident that bacterial growth is strongly influenced by the substrate's concentration. The *S. spiritovorum* metabolises extensively when there is more substrate in the soil, which enables the cell to grow and reproduce rapidly. The trend is similar to Ghosh and Mukherji (2020) where substrate concentration increased bacteria's specific growth. However, as the benzo(a)pyrene concentration was raised over 100 mg/kg, the specific growth rate rapidly reduced as a result of the benzo(a)pyrene's detrimental effects on cell development and subsequent substrate inhibition on culture growth.

The specific growth rate *S. spiritovorum* can be predicted using Monod, Haldena, Powell and Edward models as shown in Eq. 6, Eq. 7, Eq. 8 and Eq. 9, respectively. Figure 4 shows a curve-fitting on the relationship between observed (filled marker) and predicted data (red line) on the specific growth rate, μ (day^{-1}) and initial benzo(a)pyrene concentration. In the simulation, the Haldane and Edward models were most fit the curve fitting as they showed narrow convergence to the experimental data, particularly

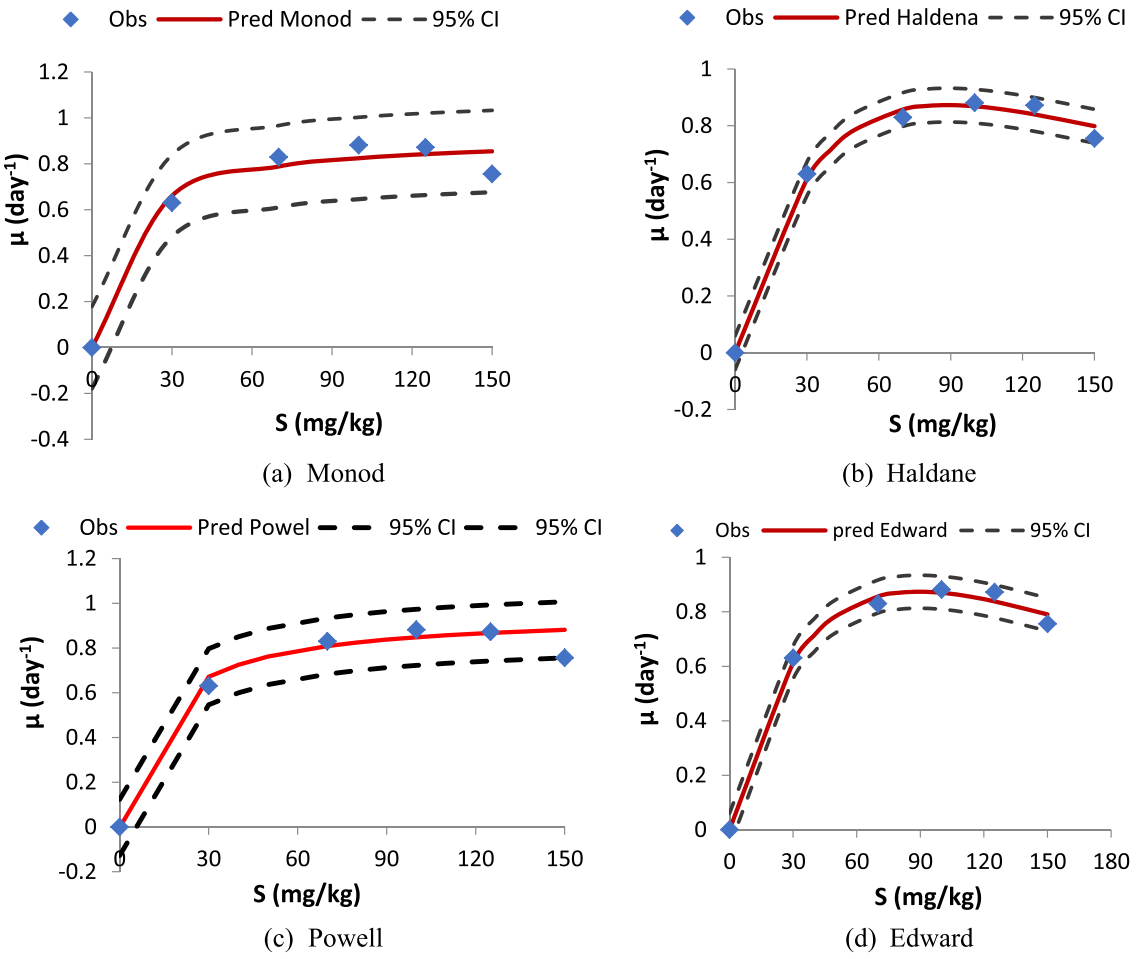

Figure 4. Curve Fitting Relationship between the Specific Growth Rate and Substrate Concentration using Monod, Haldane, Powell and Edward Models. The experimental data point (filled marker), the fit predicts (red line) and the 95% confidence intervals (black line) around the fit.

above the concentration of 70 mg/kg. In contrast, the Monod and Powel models depicted a large convergence between the growth rate of bacteria and benzo(a)pyrene concentration as they are experiencing a plateau at a concentration of more than 30 mg/kg.

The upper limit and the lower limit of 95% confidence interval were also plotted (black line) around the fitting curve. The Haldane and Edward models show narrow confidence interval for the upper and lower limit values that indicate the more precise the predicted values incomparable to the Monod and Powell models. Thus, it statistically indicated that the best-fit parameter values of the Haldane and Edward models are more precise and well suited to describe the biokinetics reaction during the development of new *S. spiritovorum* cells. Besides, Haldane and Edwards models also showed the highest R_2 values which are 0.992 and 0.993 respectively. A high R_2 value indicates the closeness between the observed and the predicted data.

The Haldane and Edward models particularly fit the inhibitory growth in which this effect was not captured in the Monod and Powell models. The models explained that the enzyme reaction that catalyses the biodegradation process was inhibited with the benzo(a)pyrene substrate when reaching the concentration of more than 30 mg/kg, indicated by the drop of specific growth rate. Substrate inhibition is a commonplace occurrence in enzyme kinetics as many enzymes are inhibited by their own substrates. It will increase velocity curves before fall with further substrate concentration increases (Reed et al., 2010). Jiang et al. (2018) also claimed that the substrate inhibition occurred when the pyrene, a four ring PAH increased from 100 to 400 mg/L in treatment using *Acinetobacter johnsonii*. In the substrate inhibition reaction, the enzyme has slowed down the reaction rate of biodegradation process, particularly once it reaches a specific substrate concentration. Generally, the enzyme reaction increases with the increase in substrate concentration, but the opposite effect occurs at large substrate concentration (Papežová et al., 2007). Substrate inhibition has certain benefits as it can control and stabilise the effect on the large concentration of end-products. Reed et al. (2010) found that the yield of a large number of end-product, such as energy (ATP), inhibited the enzyme activity, which also required the energy in the catalytic reaction. Therefore, it will reduce the demand for ATP. In this context, the end-product inhibition is also accomplished through substrate inhibition (Reed et al., 2010).

Table 4 summarises the kinetics model parameters obtained from the simulations of the Monod, Haldane, Powell and Edward models. Low values for the μ_{max} and k_s were obtained from Monod and Powell models compared to the Haldane and Edward. Low k_s and μ_{max} indicated that the bacterium only needed minimum substrate to develop new cells, and the cells were able to replicate extensively within a short time. On the other hand, the low maintenance rate, m, attained from the Powell seems unable to describe any significant effect of the cell to sustain metabolic activity. Nevertheless, the simulated data through Monod and Powell models were intolerable, while Haldane and Edward's models are more acceptable through statistics. The best-fit parameter values of the Haldane and Edward are more precise and well suited to describe the biokinetics reaction during the development of new *S. spiritovorum* cells as a narrow 95% confidence interval (CI) is obtained.

It was observed that the variability of the biokinetic model parameters reflected the dynamic characteristic of survival and bacteria growth. From the Monod model, the growth of cells is only limited by the concentration of available substrate. Meanwhile, Haldane and Edward models describe cell growth kinetics in response to the inhibitory substrate (Aiba et al., 1968). Whereas, in the Powell model, other than the use of substrate for energy for the build-up of new cells (growth), the energy was also used to maintain the metabolism. The energy is utilised to sustain the life and mortality of cells by maintaining chemical reactions in the cells (Priyadarshini et al., 2021; Muloiwa et al., 2020). In substrate inhibition condition, when the concentration of substrate exceeds the ideal values in biological system, substrate inhibition occurs, slowing the rate at which the cells develop.

3.2. Benzo(a)pyrene degradation kinetics at different initial concentrations

The trend of benzo(a)pyrene degradation by *S. spiritovorum* in sandy soil at different initial benzo(a)pyrene concentrations from 30 mg/kg to 150 mg/kg are shown in Figure 5. In general, the removal trend varied depending on the initial benzo(a)pyrene concentrations from 30, 70, 100, 125 and 150 mg/kg. A slow removal was observed at the lowest concentration, precisely 30 mg/kg, while the highest concentration depicted a rapid removal. It showed the removal rate dependent on the initial concentration of benzo(a)pyrene substrate. It was found that at the initial concentration of 30 mg benzo(a)pyrene per kg of soil (30 mg/kg), only 6% of the benzo(a)pyrene was degraded within 5 days of biological reaction. The presence of 70 mg/kg initial concentration of benzo(a) pyrene in the soil has significantly enhanced the removal of the benzo(a) pyrene to 9%. The removal increased steadily as the concentration increased and reached approximately 20% at the initial concentration of 150 mg/kg. It can be deduced that high concentration elevates the availability of benzo(a)pyrene, thus promoting a more significant contact with the *S. spiritovorum* degrading enzyme. However, as the available benzo(a)pyrene has been utilised, this growth substrate could be limited and inaccessible by the *S. spiritovorum* that resulted from the low mass-transfer rate in the solid soil phase (Mulder et al., 2001). Strong sorption between benzo(a)pyrene and soil particles which drastically decreased desorption rate can clearly be seen after day 2 of experiment. Therefore, it consequently limits the degradation of the benzo(a)pyrene by the *S. spiritovorum*. Furthermore, substrate inhibition could be another reason that prevented the substrate utilisation rate, as priorly discussed.

A high molecular weight PAH (HMW-PAH) with four and more benzene rings such as benzo(a)pyrene, normally showed low capabilities to catabolize by most of the microorganisms (Li et al., 2021). These categories of PAHs can strongly adsorb in soil, will be recalcitrant in the environment, and become less favourable as compared to LMW-PAH which tend to dissolve in water due to high bioavailability (Warshawsky et al., 2007; Sanghvi, 2005). The efficiency and rate of PAH biodegradation or its kinetics have significantly related to the bioavailability and bioaccessibility of PAH (Deary et al., 2016; Rostami and Juhasz, 2013). Contaminated sites with a high bioavailability index in which biodegradation rate is lower than the mass transfer rate, is more

Table 4. Kinetics model parameters of *S. spiritovorum* growth rate of monod, haldane, powell and edward models.

Parameter Model	Maximum Specific Growth Rate, μ_{max} (day^{-1})	Half Saturation Constant, k_s (mg/kg)	Substrate Inhibition Coefficient, k_i (mg/kg)	Maintenance Rate, m (day^{-1})	K	R^2	CI
Monod Model	0.922	11.874	-	-	-	0.971	[0.149 0.190]
Haldane Model	2.28	84.66	92.82	-	-	0.992	[0.052 0.104]
Powell Model	0.956	12.672	-	0.002	-	0.964	[0.080 0.136
Edward Model	2.011	63.02	182.60	-	406.83	0.993	[0.038 0.071]

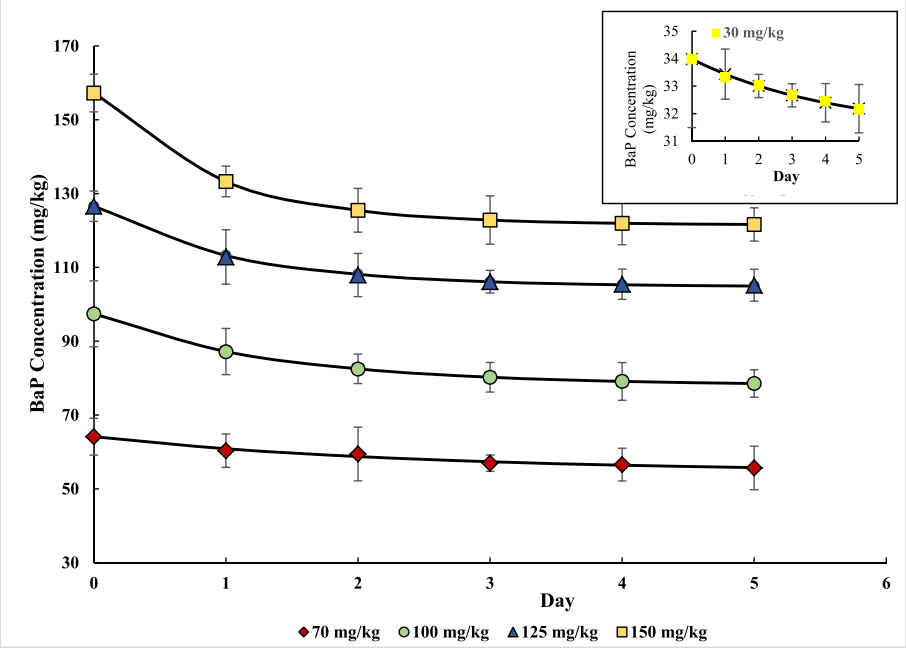

Figure 5. Degradation of Benzo(a)pyrene at Different Initial Benzo(a)pyrene Concentrations. The marker represents the mean value of benzo(a)pyrene from the experiment (n = 3) and their standard deviations, whereas the lines are the predicted value from the model.

suitable for bioremediation. However, mass transfer rates will gradually reduce as concentration gradients within the soil decrease because of the increase in the adsorption process. On the other hand, contaminated sites with a low bioavailability index might need additional treatments to solubilise and raise up the concentrations of the contaminants in the water (Haws et al., 2006). Furthermore, other than bioavailability effect, substrate inhibition, enzyme activities and terminal electron acceptor have also play a major role in remediating PAHs contaminated sites (Priyadarshini et al., 2021; Mu et al., 2022).

Benzo(a)pyrene degradation was model using a fourth order Runge-Kutta numerical analysis as an Excel spreadsheet shown in Figure 6. This numerical algorithm predicts the value of benzo(a)pyrene concentration (C_{pred}) by integrating the ordinary differential equation (ODE) of the Haldane substrate utilisation model as expressed in Eq. (10). Figure 7 shows the framework to describe substrate (BaP) utilisation in sandy soil by *S. spiritovorum*. The k_b describes the available substrate for the microorganism as the benzo(a)pyrene desorb from the soil. At the same time, the benzo(a)pyrene could also be sorbed again on the soil particles. However, desorption is expected to be predominant over the sorption; therefore, k_b highly represents the desorption process. The q_{max}, X and k_b are determined through fitting the kinetic parameters to the model by numerical iteration, while k_i and k_s are set as constant based on the value obtained in the curve fitting *S. spiritovorum* growth model. The model was run based on the predefined initial benzo(a)pyrene substrate concentration with the kinetic parameters for of k_s of 84.66 mg/kg, k_i of 92.82 mg/kg and any random value of q_{max}, X and k_b.

Table 5 summarises the value of the best fit model from the curve fitting of biokinetics parameters on the degradation of benzo(a)pyrene by *S. spiritovorum* at different concentration. The values of fitting kinetic parameters of the benzo(a)pyrene biodegradation attained in this simulation can elucidate the understanding of the physico-biological interaction of the soil-PAH and the process performance. Noting again, the utilisation of benzo(a) pyrene is highly dependent on substrate concentration. The maximum substrate utilisation rate (q_{max}) was found to increase with the increasing benzo(a)pyrene concentration. Similarly, the biomass concentration (X) also increases with benzo(a)pyrene concentration.

When present at high concentrations, benzo (a)pyrene substrate offers more substrates for the growth of bacteria, which promotes rapid utilisation of the substrate. The higher utilisation of substrate reflects more removal of the substrate from the soil. This substrate utilisation rate has been affected by the limitation of the substrate in which it is a function of the half-saturation constant (k_s). The half-saturation constant can be described as the concentration of the available substrate when half of its maximum utilisation rate is reached.

Figure 8 shows the relationship between substrate utilisation rate, bacterial specific growth rate and substrate concentration. It clearly be seen that the uptake and utilisation increase with the specific growth rate of *S. spiritovorum*. Benzo(a)pyrene substrate at high concentration can ease its utilisation and uptake as the growth substrate promotes a greater utilisation/degradation rate. However, the rate of benzo(a)pyrene degraded reduce as it reached the concentration of more than 120 mg/kg. There are many reasons that limit the biodegradation of benzo(a) pyrene other than substrate inhibition factor. Boopathy (2000) discussed in detail factors limiting bioremediation approach which can be categoried into seven (i) microbials (enzyme inhibition and toxic metabolites (ii) environment (depletion of preferable substrate and nutrient) (iii) substrate (low concentration, solubility and toxicity of substrate, (iv) treatment aerobic vs anaerobic (availability of electron acceptor, redox reaction) (v) growth substrate vs co-metabolite (type of contaminants, carbon source) (vi) availability of substrate (sorption, desorption, humic matter) and (vii) limitation in mass transfer (diffusion of nutrient, oxygen, solubility in water phase).

The value of the desorption coefficient of the benzo(a)pyrene (k_b) from the soil into liquid phase corresponded to the hydrophobic properties of HMW-BaP, sorption of BaP on the matrix particle of the sand and benzo(a)pyrene concentration. Generally, the desorption coefficient (k_b) is almost constant at all benzo(a)pyrene concentrations. Low value of k_b is observed at concentration below 70 mg/kg while the value is slightly increased at benzo(a)pyrene above 70 mg/kg Viamajala et al. (2007) observed the solubilisation rate of PAHs increased with the increase in PAHs concentration. Additionally, it also depends on the type of PAH. It is challenging to dissolve benzo(a)pyrene in the aqueous phase since it is a hydrophobic contaminant. Only when the contaminant is easily available to the water's advection flow, they can be taken up by microbes straightaway (Haws et al., 2006). Bacteria, known to only utilise soluble substrate, might not be accessible to utilise the substrate inside the soil

Sole Substrate Parameter Estimation (BaP SS)

$dS/dt = k_b S - (q_{max} SX)/(k_s + S + (S^2/k_i)$

LET,

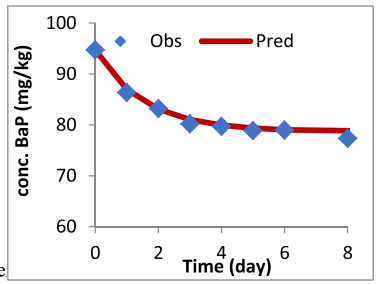

q_m	3.3362	mg/kg-d	Constant	kb	0.583	Fitting Parameter	
k_s	84.6600	mg/kg	Constant	ki	92.82	Fitting Parameter	
X	40.2052	Biomass/kg	Fitting Parameter				
C_0	97.200	mg/kg	Constant	Mean of y	85.140000000	critical t	12.7062
dt	1	day	Constant	df	1.0000 34	CI	8.11940
				SE of y	0.639010777		
				R2	0.9987		

			$C_{i(pred)} = C_o - 1/6\,[K1 + 2K2 + 2K3 + K4]dt$										SSE	
				dC/dt	K1= $hf(t_n, C_n)$	K2=$hf(t_n+0.5h, C_n + 0.5K1)$		K3=$hf(t_n+0.5h, C_n+0.5K2)$		K4=$hf(t_n+h, C_n+K3)$		K1+2K2+2K3+K4	(C_{obs} - C_{pre})	(C_{obs} - C_{pre})^2
No.	Time	C_{exp}	C_{pred}		K1	Cn + 0.5K1	K2	Cn + 0.5K2	K3	Cn + K3	K4		Error	Error^2
1	0	97.200000000	97.200000000	10.73285 66	10.7329	102.5664	10.7329	102.5664	10.7329	107.9329	10.7329	64.3971	0.0000	0.0000
2	1	86.200000000	86.4671	4.353617965	4.3536	88.6440	4.3536	88.6440	4.3536	90.8208	4.3536	26.1217	-0.2671	0.0714

Figure 6. Spreadsheet Modeling of Benzo(a)pyrene Degradation using Runga-Kutta Numerical Analysis.

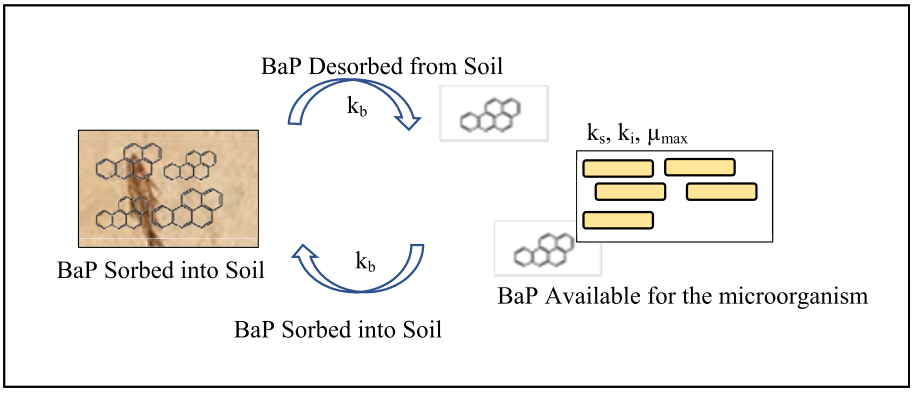

Figure 7. Framework to describe benzo(a)pyrene substrate utilisation in sandy soil by *S. spiritovorum*.

Table 5. Biokinetic parameters by *S. spiritovorum* at Different Initial Concentration of benzo(a)pyrene.

C_o mg/kg	X mg/kg	q_{max} mg/kg/d	k_s mg/kg	k_b day^{-1}	k_i mg/kg	R^2	SSE
34.903	2.768	20.856	84.66	0.456	92.82	0.991	0.0164
65.848	2.266	33.159	84.66	0.442	92.82	0.975	0.951
94.409	2.8753	42.033	84.66	0.53	92.82	0.999	0.005
126.180	2.939	55.444	84.66	0.52	92.82	0.999	0.2781
157.254	3.199	60.3441	84.66	0.53	92.82	0.999	0.202

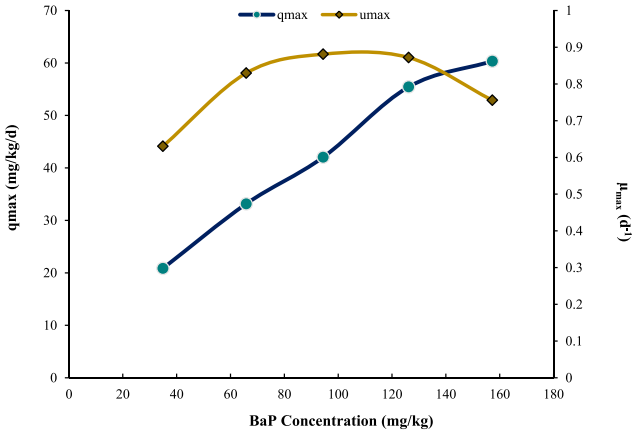

Figure 8. Substrate (BaP) utilisation rate (qmax) and specific growth rate of *S. spiritovorum* for BaP concentrations from 0 to 157 mg/kg.

pore volumes. A low concentration of solubilising benzo(a)pyrene in the water phase is due to the low desorption rate, limiting the benzo(a) pyrene degradation. Hence these have resulted in incomplete remediation of the contaminated soil by bacteria biological agents.

3.3. Simulation of Benzo(a)pyrene biodegradation

Figure 9 shows the simulation of benzo(a)pyrene biodegradation using the biokinetic parameters of the degradation model in which an insert depicts a high concentration. It was observed that the BaP will remain in the soil at concentration of 0.043 mg/kg and 0.0161 mg/kg from its initial concentration of 0.18 mg/kg and 0.685 mg/kg, respectively. The simulation used initial concentration of benzo(a)pyrene found in marine sediment at Malaysia (Sakari and Zakaria, 2013) and agricultural soil in Poland (Maliszewska-Kordybach et al., 2009). According to Department of Environment Malaysia (DOE, 2009), the allowable limit of benzo(a)pyrene in soil for residential development is 0.015 mg/kg. Meanwhile, the Canadian Council of Ministers of the Environment (CCME, 2010) lays 0.1 mg/kg benzo(a)pyrene for agricultural soil. Environmental New Zeneli et al. (2019) (ENZ) allows 0.027 mg/kg benzo(a)pyrene for the agricultural purposes. The benzo(a)pyrene is set to be within the maximum value of 0.7–11 mg/kg in industrial soil (Canadian Council of Ministers of the Environment, 2010; DOE, 2009; Environmental New Zealand, 2006).

Based on the guideline, it was found benzo(a)pyrene at low concentration has potential to be treated with the *S. spiritovorum* as it can reach the allowable limit for agricultural soil and almost comply with residential soil. However, when the benzo(a)pyrene presence at high concentration specifically from coal tar contaminated site (61–143 mg/kg) from data obtained by Lors et al. (2012) and Lee et al. (2001) the soil is strictly considered unsuitable for residential and agriculture purposes. Besides, the development of industry is also not allowed on this brownfield soil since the exceeded the permissible limit. Therefore, through the developed model, the authority can predict the remaining concentration of benzo(a)pyrene prior treatment is applied. This will help in decision making on the most practical and effective strategies in remediation PAH polluted soil, particularly benzo(a)pyrene.

4. Conclusion

In this study, the biodegradation kinetics of benzo(a)pyrene, a HMW-PAH, in contaminated soil by *S. spiritovorum* was evaluated and modelled. Through batch experiments, the depletion of benzo(a)pyrene as model

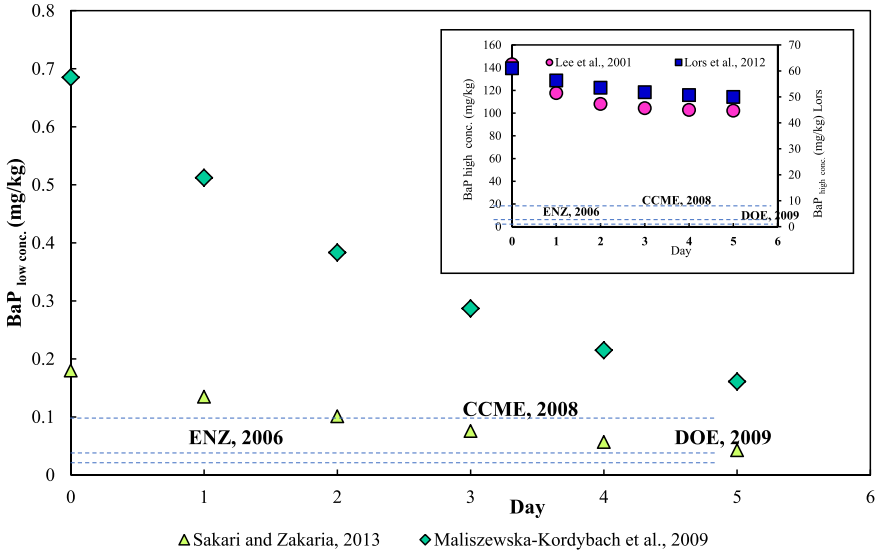

Figure 9. Simulation on biodegradation of benzo(a)pyrene at various initial concentrations.

substrate over time was analysed to derive biokinetic coefficients, which are subsequently generated by fitting the experimental data to biokinetics model. As opposed to Monod and Powel models, Haldane and Edward provide a high correlation ($R > 0.99$) with significantly slender confidence interval region that best describe the biokinetics reaction of benzo(a)pyrene degradation. The Haldane and Edward equation model determines if a substrate is toxic, that can slow down the microbial growth and severely affect the ability to degrade the benzo(a)pyrene. This substrate inhibition occurs when substrate concentration is increased which thus decreased in substrate utilization rate. The best biokinetics parameters value of Haldane model for benzo(a)pyrene degradation by *S. spiritovorum* is $\mu max = 2.28\ day^{-1}$, $ks = 84.66$ mg/kg and $ki = 92.82$ mg/kg. Overall, the finding of this study shows that the presence of *S. spiritovorum* in contaminated soil capable of degrading the benzo(a)pyrene but the substrate of high concentration will result in self-inhibition in biodegradation process. In order to remediate soil contaminated with benzo(a)pyrene, it is possible to advise studying an enzymatic process utilising *S. spiritovorum*. Additionally, it would be best to investigate analytical and kinetics models that incorporate the cometabolism effect utilising a mixture of PAHs.

Declarations

Author contribution statement

Salina Alias: Conceived and designed the experiments; Performed the experiments; Analyzed and interpreted the data; Contributed reagents, materials, analysis tools or data; Wrote the paper.

Megawati Omar: Contributed reagents, materials, analysis tools or data.

Noor Hana Hussain: Conceived and designed the experiments.

Nor Amani Filzah Mohd-Kamil: Performed the experiments.

Suhaimi Abdul-Talib: Conceived and designed the experiments; Contributed reagents, materials, analysis tools or data.

Funding statement

This research did not receive any specific grant from funding agencies in the public, commercial, or not-for-profit sectors

Data availability statement

Data included in article/supp. material/referenced in article.

Declaration of interest's statement

The authors declare no conflict of interest.

Additional information

No additional information is available for this paper.

Acknowledgements

The authors are grateful to the Universiti Teknologi MARA, Malaysia, for the facilities support in this research works.

References

Aiba, S., Shoda, M., Nagatani, M., 1968. Kinetics of product inhibition in alcohol fermentation. Biotechnol. Bioeng. 10, 845–864.

Alias, S., Omar, M., Hussain, N.H., Abdul-Talib, S., 2012. Zero valent iron particles for the degradation of polycyclic aromatic hydrocarbons in contaminated soil. Adv. Mater. Res. 587, 111–115.

Balseiro-Romero, M., Monterroso, C., Kidd, P.S., Lu-Chau, T.A., Gkorezis, P., Vangronsveld, J., Casares, J.J., 2019. Modelling the ex situ bioremediation of diesel-contaminated soil in a slurry bioreactor using a hydrocarbon-degrading inoculant. J. Environ. Manag. 246, 840–848.

Boopathy, R., 2000. Factors limiting bioremediation technologies. Bioresour. Technol. 74 (1), 63–67.

Canadian Council of Ministers of the Environment, 2010. Canadian Soil Quality Guidelines : Carcinogenic and Other Polycyclic Aromatic Hydrocarbons.

Dai, C., Han, Y., Duan, Y., Lai, X., Fu, R., Liu, S., Leong, K.H., Tu, Y., Zhou, L., 2022. Review on the contamination and remediation of polycyclic aromatic hydrocarbons (PAHs) in coastal soil and sediments. Environ. Res. 205 (March 2021).

Deary, M.E., Ekumankama, C.C., Cummings, S.P., 2016. Development of a novel kinetic model for the analysis of PAH biodegradation in the presence of lead and cadmium co-contaminants. J. Hazard Mater. 307, 240–252.

Department of Environment Malaysia, 2009. Contaminated Land Management and Control Guidelines No. 1: Malaysian Recommended Site Screening Levels for Contaminated Land, pp. 1–66. https://www.doe.gov.my/portalv1/wp-content/uploads/Contaminated-Land-Management-and-Control-Guidelines-No-1_Malaysian-Recommended-Site-Screening-Levels-for-Contaminated-Land.pdf.

Ghosh, P., Mukherji, S., 2020. Modeling growth kinetics and carbazole degradation kinetics of a Pseudomonas aeruginosa strain isolated from re fi nery sludge and uptake considerations during growth on carbazole. Sci. Total Environ. 738, 140277.

Gonçalves, R., Scholze, M., Ferreira, A.M., Martins, M., Correia, A.D., 2008. The joint effect of polycyclic aromatic hydrocarbons on fish behavior. Environ. Res. 108 (2), 205–213.

Haws, N.W., Ball, W.P., Bouwer, E.J., 2006. Modeling and interpreting bioavailability of organic contaminant mixtures in subsurface environments. J. Contam. Hydrol. 82 (3–4), 255–292.

Hibi, A., Kumano, Y., 2017. Sphingobacterium spiritivorum bacteremia due to cellulitis in an elderly man with chronic obstructive pulmonary disease and congestive heart failure: a case report. J. Med. Case Rep. 11 (1), 1–5.

Janbandhu, A., Fulekar, M.H., 2011. Biodegradation of phenanthrene using adapted microbial consortium isolated from petrochemical contaminated environment. J. Hazard Mater. 187 (1–3), 333–340.

Jiang, Y., Zhang, Z., Zhang, X., 2018. Co-biodegradation of pyrene and other PAHs by the bacterium Acinetobacter johnsonii. Ecotoxicol. Environ. Saf. 163 (April), 465–470.

Jørgensen, K.S., Puustinen, J., Suortti, A.M., 2000. Bioremediation of petroleum hydrocarbon-contaminated soil by composting in biopiles. Environ. Pollut. 107 (2), 245–254.

Lambiase, A., Rossano, F., Del Pezzo, M., Raia, V., Sepe, A., de Gregorio, F., Catania, M.R., 2009. Sphingobacterium respiratory tract infection in patients with cystic fibrosis. BMC Res. Notes 2, 262.

Lammert, J., 2007. Techniques in Microbiology, pp. 1–223.

Lee, P.H., Ong, S.K., Golchin, J., Nelson, G.L., 2001. Use of solvents to enhance PAH biodegradation of coal tar-contaminated soils. Water Res. 35 (16), 3941–3949.

Li, M., Yin, H., Zhu, M., Yu, Y., Lu, G., Dang, Z., 2021. Biodegradation of mixed PAHs by highly efficient microbial consortium QY1. J. Environ. Sci. 107, 65–76.

Liang, C., Ye, Q., Huang, Y., Wang, Y., Zhang, Z., Wang, H., 2022. Shifts of the new functional marker gene (pahE) of polycyclic aromatic hydrocarbons (PAHs) degrading bacterial population and its relationship with PAHs biodegradation. J. Hazard. Mater. 437 (June).

Lors, C., Damidot, D., Ponge, J.F., Périé, F., 2012. Comparison of a bioremediation process of PAHs in a PAH-contaminated soil at field and laboratory scales. Environ. Pollut. 165, 11–17.

Lu, C., Hong, Y., Stephen, E., Liu, J., Tsang, D.C.W., 2021. Bacterial community and PAH-degrading genes in paddy soil and rice grain from PAH-contaminated area. Applied Soil Ecology Journal 158 (September 2020), 1–10.

Maliszewska-Kordybach, B., Smreczak, B., Klimkowicz-Pawlas, A., 2009. Concentrations, sources, and spatial distribution of individual polycyclic aromatic hydrocarbons (PAHs) in agricultural soils in the Eastern part of the EU: Poland as a case study. Sci. Total Environ. 407 (12), 3746–3753.

Mu, J., Chen, Y., Song, Z., Liu, M., Zhu, B., Tao, H., Bao, M., Chen, Q., 2022. Effect of terminal electron acceptors on the anaerobic biodegradation of PAHs in marine sediments. J. Hazard. Mater. 438 (June).

Mulder, H., Breure, A.M., Rulkens, W.H., 2001. Prediction of complete bioremediation periods for PAH soil pollutants in different physical states by mechanistic models. Chemosphere 43 (8), 1085–1094.

Muloiwa, M., Nyende-Byakika, S., Dinka, M., 2020. Comparison of unstructured kinetic bacterial growth models. S. Afr. J. Chem. Eng. 33 (July), 141–150.

Othman, N., Hussain, N., Abdul-Talib, S., 2010. Degradation of Polycyclic Aromatic Hydrocarbon by Pure Strain Isolated from Municipal Sludge: Synergistic and Cometabolism Phenomena. International Conference on Environment, 2010(Icenv).

Papežová, K., Němec, T., Chaloupková, R., Glatz, Z., 2007. Study of substrate inhibition by electrophoretically mediated microanalysis in partially filled capillary. J. Chromatogr. A 1150 (1–2), 327–331.

Perera, F., Tang, D., Whyatt, R., Lederman, S.A., Jedrychowski, W., 2005. DNA damage from polycyclic aromatic hydrocarbons measured by benzo[a]pyrene-DNA adducts in mothers and newborns from northern manhattan, the world trade center area, Poland, and China. Cancer Epidemiology, Bomarkers & Prevention 14 (3), 709–714.

Plísková, M., Vondrácek, J., Vojtesek, B., Kozubík, A., Machala, M., 2005. Deregulation of cell proliferation by polycyclic aromatic hydrocarbons in human breast carcinoma MCF-7 cells reflects both genotoxic and nongenotoxic events. Toxicol. Sci. 83 (2), 246–256.

Priyadarshini, A., Sahoo, M.M., Raut, P.R., Mahanty, B., Sahoo, N.K., 2021. Kinetic modelling and process engineering of phenolics microbial and enzymatic biodegradation: a current outlook and challenges. J. Water Proc. Eng. 44. Elsevier Ltd.

Reed, M.C., Lieb, A., Nijhout, H.F., 2010. The biological significance of substrate inhibition: a mechanism with diverse functions. Bioessays 32 (5), 422–429.

Rostami, I., Juhasz, A.L., 2013. Bioaccessibility-based predictions for estimating PAH biodegradation efficacy - comparison of model predictions and measured endpoints. Int. Biodeterior. Biodegrad. 85, 323–330.
Sahar, N., Shahid, M., Ali, A., 2020. A case of Sphingobacterium spiritivorum bacteremia and literature review. Infect. Dis. Clin. Pract. 28 (1), 7–9.
Sakari, M., Zakaria, M.P., 2013. Distribution, characterization and origins of polycyclic aromatic hydrocarbons (PAHs) in surficial sediment of penang, Malaysia: the presence of fresh and toxic substances. World Appl. Sci. J. 23 (11), 1481–1488.
Sanghvi, S., 2005. Bioremediation of polycyclic aromatic hydrocarbon contamination using Mycobacterium vanbaalenii. Basic Biotechnology EJournal 445, 1–7.
Saravanakumar, K., Sivasantosh, S., Sathiyaseelan, A., Wang, M., 2022. Impact of Benzo [a] Pyrene with Other Pollutants Induce the Molecular Alternation in the Biological System : Existence , Detection , and. 304(March).
Smu, W., Sydow, M., Zabielska-matejuk, J., Kaczorek, E., 2020. Bacteria involved in biodegradation of creosote PAH – a case study of long- term contaminated industrial area. Ecotoxicol. Environ. Saf. 187, 109843.
Su, D., Pu, Y., Gong, C., He, Z., 2021. Application of cold-adaptive Pseudomonas sp . SDR4 and Mortierella alpina JDR7 co-immobilized on maize cob in remediating PAH-contaminated freeze-thawed soil. Environmental Advances 4 (March), 100063.
Sun, Z., Wang, L., Yang, S., Xun, Y., Zhang, T., Wei, W., 2022. Thermally enhanced anoxic biodegradation of polycyclic aromatic hydrocarbons (PAHs) in a highly contaminated aged soil. J. Environ. Chem. Eng. 10 (2).
Thakur, T.K., Dutta, J., Upadhyay, P., Patel, D.K., Thakur, A., Kumar, M., Kumar, A., 2022. Assessment of land degradation and restoration in coal mines of central India: a time series analysis. Ecol. Eng. 175 (October 2021).
Tronel, H., Plesiat, P., Ageron, E., Grimont, P.A.D., Minjoz, Ã.J., Ente, Â., 2003. Bacteremia Caused by a Novel Species of Sphingobacterium. European Society of Clinical Microbiology and Infectious Diseases, pp. 8–10.
USEPA, 2007a. Method 3546. Microwave Extraction, pp. 1–13. ReVision, February.
USEPA, 1986. Method 8310: Polycyclic Aromatic Hydrocarbon. September, pp. 1–13.
USEPA, 2003. METHOD 8000C: Determinative Chromatographic Separations.
USEPA, 2007. METHOD 3500C - Organic Extraction and Sample Preparation, pp. 1–19. Issue February.
Viamajala, S., Peyton, B.M., Richards, L.A., Petersen, J.N., 2007. Solubilization, solution equilibria, and biodegradation of PAH's under thermophilic conditions. Chemosphere 66 (6), 1094–1106.
Wang, X., Priya Veeraraghavan, V., Krishna Mohan, S., Lv, F., 2021. Anticancer and immunomodulatory effect of rhaponticin on Benzo(a)Pyrene-induced lung carcinogenesis and induction of apoptosis in A549 cells. Saudi J. Biol. Sci. 28 (8), 4522–4531.
Warshawsky, D., LaDow, K., Schneider, J., 2007. Enhanced degradation of benzo[a] pyrene by Mycobacterium sp. in conjunction with green alga. Chemosphere 69 (3), 500–506.
Wick, A., Haus, N., Sukkariyah, B., Haering, K., Daniels, W., 2011. Remediation of PAH-contaminated soils and sediments: a literature review. Virginia Polytecnic 1–102. http://www.landrehab.org/UserFiles/DataItems/66647A54537164594C6F513D/Virginia Tech PAH Remediation Lit Review 2011.pdf.
Zeneli, A., Kastanaki, E., Simantiraki, F., Gidarakos, E., 2019. Monitoring the biodegradation of TPH and PAHs in refinery solid waste by biostimulation and bioaugmentation. J. Environ. Chem. Eng. 7 (3).